Heat and Mass Transfer Effects on Peristaltic Transport of Eyring Powell Fluid Through an Inclined Non-uniform Channel

Manjunatha Gudekote, Rajashekhar Choudhari, Prathiksha, Balachandra Hadimani*, Hanumesh Vaidya, Kerehalli Vinayaka Prasad and Jyothi Shetty

***Abstract*—The present investigation emphasizes a new attempt at the peristaltic mechanism of Eyring Powell fluid through a non-uniform channel. The flow is analyzed in the presence of wall properties under variable liquid properties, and the mathematical problem for the flow is developed. The channel walls are subjected to slip conditions with low Reynolds number, and long wavelength approximations are employed to simplify the nonlinear governing equations. The nonlinear governing equations are normalized using relevant non-dimensional parameters, and the solutions are obtained with the help of the regular perturbation technique. The influence of pertinent physical parameters of interest (velocity, temperature, concentration, and streamlines) are represented graphically. The investigations reveal that the material parameters and elastic parameters of the Eyring Powell fluid model strongly affect the velocity and temperature profiles. The model shows the opposite behaviour in the material parameters A and B in velocity and temperature profiles.**

***Index Terms*—Eyring Powell Fluid, Wall Properties, Variable Liquid Properties, Non-Uniform Channel**

NOMENCLATURE

a	Radius of the channel
b	Wave amplitude
c	Wave speed
g	Acceleration due to gravity
Re	Reynolds number
w	Radial velocity
u	Axial velocity
x	Non-dimensional axial distance
y	Non-dimensional radial distance

GREEK SYMBOLS

θ	Non-dimensional temperature
ϕ	Non-dimensional concentration
δ	Wave number
α	Inclination angle of the channel
$\dot{\gamma}$	Strain rate
λ	Wavelength

Manuscript received August 03, 2022; revised February 27, 2023.

Dr Manjunatha Gudekote is an Associate Professor in the Department of Mathematics, Manipal Institute of Technology, Manipal Academy of Higher Education, Manipal, India (email:manjunatha.g@manipal.edu).

Dr Rajashekhar Choudhari is an Assistant Professor in the Department of Mathematics, Manipal Institute of Technology Bengaluru, Manipal Academy of Higher Education, Manipal, India (email:rv.choudhari@manipal.edu).

Ms Prathiksha is a Research Scholar in the Department of Mathematics, Manipal Institute of Technology, Manipal Academy of Higher Education, Manipal, India (email:sanil.prathiksha@learner.manipal.edu).

Dr Balachandra Hadimani (*Corresponding Author) is an Assistant Professor in the Department of Mathematics, Manipal Institute of Technology, Manipal Academy of Higher Education, Manipal, India (email:bs.hadimani@manipal.edu).

Dr Hanumesh Vaidya is an Associate Professor in the Department of Mathematics, Vijayanagara Sri Krishnadevaraya University, Ballary, India (email:hanumeshvaidya@gmail.com).

Dr Kerehalli Vinayaka Prasad is a Professor in the Department of Mathematics, Vijayanagara Sri Krishnadevaraya University, Ballary, India (email:prasadkv2007@gmail.com).

Dr Jyothi Shetty is an Assistant Professor in the Department of Mathematics, Manipal Institute of Technology Bengaluru, Manipal Academy of Higher Education, Manipal, India (email:shetty.jyothi@manipal.edu).

I. Introduction

PERISTALSIS is a muscle-controlled flow that resembles the circulatory system. When a progressive wave of area passes through a distensible tube, peristalsis flow occurs. Walls of the medium (tube/channel) are subjected to contraction and expansion. Peristaltic flow is a natural flow that uses periodic wavelike sinusoidal oscillations to carry out its functions. Contents of the vessels are forced to move forward as they pass along the walls. This mechanism is essential in understanding the flow of biofluids such as blood, urine, and tears in the human body. Peristaltic flow occurs widely in the functioning of the ureter, bile transport, blood vessels, and so on. Latham [1] first investigated the mechanism of peristaltic transport of Newtonian viscous incompressible fluid through the ureter. Further, Shapiro et al. [2] developed a mathematical model for peristaltic pumping based on low Reynolds number and long wavelength approximations for viscous incompressible fluid flow in a two-dimensional channel. Slip, and heat transmission was studied by Hayat et al. [3] for peristaltic flow in an irregular channel. It has been seen that in a quantitative sense, the velocity and thermal slip parameters have identical impacts on the pressure rise. The influence of a radially varying applied magnetic field on the peristaltic transport of a Carreau-Yasuda fluid via a curved conduit was shown by Shehzad et al. [4]. The Runge-Kutta fourth-order technique is used to solve the governing nonlinear equations under nonlinear boundary conditions. Effects of various parameters on the variables of interest were analysed using graphs. According to this study, increasing the intensity of the applied magnetic field and velocity slip parameter decreases the maximum fluid velocity. Peristalsis of Walters-B fluid in a compliant wall channel was studied by Javed et al. [5] in the presence of velocity and thermal slip factors. Manjunatha and Rajashekhar [6] conducted the study of peristaltic transport on Casson fluid with slip effects. The focus of the study was on the peristaltic blood transport in an elastic tube and its flow characteristics. It was seen that the slip and porous parameters had the opposite

behaviour on flow rate, concluding that flux in a flexible tube reduces as the slip parameter grows, and increases as the porous parameter increases. Casson fluid peristaltic pumping in a heated permeable channel with changeable fluid characteristics was examined by Manjunatha et al. [7]. Variable viscosity and slip parameters were studied by Vaidya et al. [8] in a convectively heated porous channel for the peristaltic transport of Rabinowitch fluid.

Heat transmission in biological fluids significantly impacts our knowledge of fluid dynamics. Conduction, radiation, convection, and evaporation are the four heat exchange methods used by the body to keep temperature stable. For these processes to work, conduction must transfer heat from a high concentration to a low concentration. As a result, the pace of heat exchange processes varies depending on the temperature and environmental factors. Based on the use of heat transfer theory, research was conducted by Ellahi et al. [9] to determine the influence of heat and mass transfer on peristaltic transport in non-uniform channels using rectangular tubes. An investigation of the effects of heat transfer in the peristalsis-induced flow of a viscous electrically conducting fluid in an asymmetric channel in the presence of Hall and Ion-slip effects at the borders was undertaken by Hussain et al. [10]. The numerical solutions for the MHD flow of heat transfer of incompressible second-grade fluid on a stretching sheet channel were obtained by Faisal and Mubarak [11]. Velocity and thermal slip were considered in the investigation. Manjunatha et al. [12] investigated the heat and mass transfer effect on the peristalsis of Jeffery fluid in a non-uniform porous channel with variable viscosity and thermal conductivity. Another study explored the effect of heat transfer on the peristaltic movement of Casson fluid in an axisymmetric porous tube by Vaidya et al. [13]. Ahmed et al. [14] examined the mixed convection peristalsis of hybrid nanomaterial flow in the thermally active symmetric channel. Rajashekhar et al. [15] recently established a theoretical model to trigger electro-osmosis by peristalsis in a microchannel with changing liquid characteristics and wall properties. For the series solutions, the perturbation method is used. The velocity and temperature profiles are enhanced when the variable viscosity is increased.

Mittra and Prasad [16] investigated the influence of wall characteristics on peristalsis. An elastic or viscoelastic wall is addressed in the two-dimensional analysis of peristalsis. Hayat et al. [17] have created a novel mathematical model to investigate the influence of heat and mass transfer on peristaltic flow in a curved channel with compliant walls. Mustafa et al. [18] studied the peristalsis of nanofluids in compliant media using long wavelength and low Reynolds number approximations. With an increase in temperature and concentration, the power of Brownian motion effects becomes more pronounced. In addition, when Brownian motion and thermophoresis parameters rise, the heat transfer coefficient falls. Mariyam et al. [19] studied the influence of wall characteristics on the peristalsis of non-Newtonian fluid. Further, Hina et al. [20] examined the impact of wall features and heat/mass transmission on the movement of pseudoplastic fluid along a circular conduit. MHD peristaltic flow of Eyring Powell nanofluid with convective and noslip conditions was studied by Nisar et al. [21]. In the curved channel peristaltic transport of Sisko fluid, variable viscosity was studied by Tanveer et al. [22]. The perturbation method is applied to obtain the numerical solutions. This research shows that increasing viscosity lowers flow velocity and temperature, whereas increasing viscous dissipation parameter increases the fluid temperature. The peristaltic process of Jeffery fluid in a non-uniform porous channel was studied by Manjunatha et al. [23]. The bolus size grows as the variable viscosity parameter rises, and so do the fluid velocity and temperature. Varying transport characteristics on Casson nanofluids were studied by Prasad et al. [24]. For the solutions, the Keller box approach was used. It turns out, according to the findings, that increasing viscosity has the opposite effect on flow velocity and temperature. The peristaltic flow of Ree-Eyring fluid across a uniform conduit with variable liquid characteristics was studied by Rajashekhar et al. [25]. There was a noticeable improvement in velocity and creation of trapped bolus as the temperature rose due to the changing viscosity and thermal conductivity. Electro-osmotic peristaltic flow in a microchannel with varying liquid characteristics was studied by Rajashekhar et al. [26] in depth. Streamlines and fluid temperature were solved using the perturbation method. It was found that increasing the variable viscosity positively affected fluid velocity and temperature, whereas increasing the variable thermal conductivity positively affected liquid temperature.

The Eyring Powell model was developed by Powell and Eyring [27]. Based on the theory of gas dynamics rather than actual data, this model is more appropriate than other non-Newtonian models. This model reduces Newtonian flow characteristics in both high and low shear rates. By examining this model, Akbar and Nadeem [28] were the first to investigate the influence of heat and mass transfer on the peristaltic flow of Eyring Powell fluid. Standard perturbation and fire techniques were used to evaluate analytical and numerical solutions. Abbasi et al. [29] also studied Eyring Powell fluid model peristaltic transport using long wavelength and low Reynolds number approximations. Hina [30] investigated the peristaltic transport of Eyring Powell fluid in a complaint wall channel with heat/mass transfer. An investigation of Eyring Powell fluid flow in a curved channel was conducted by Farooq et al. [31]. Recently, Elniel et al. [32] investigated Eyring Powell fluid MHD flow on an inclined porous plate in the presence of shear stress for both lift and draining flow.

To the author's knowledge, peristaltic transport of Eyring Powell fluid under the impact of varying liquid characteristics and wall properties through the inclined non-uniform channel has not been explored based on the literature described above.To bridge this knowledge gap, current work has been done. the nonlinear governing equations are simplified under long wavelength and low Reynolds number approximations. In addition, the classical perturbation technique is used to solve these equations concerning heat transport and the Eyring Powell fluid with changeable liquid properties. The graphical representation is used to demonstrate the influence of model parameters.

II. Formulation of the Problem

Consider an incompressible viscous fluid flowing through an inclined non-uniform channel. Non-Newtonian Eyring Powell Fluid governs the flow. The varying viscosity and variable thermal conductivity are taken into account. The equations governing the flow are written as follows:

$$\frac{\partial u'}{\partial x'} + \frac{\partial w'}{\partial y'} = 0, \tag{1}$$

$$\rho\left[\frac{\partial u'}{\partial t'} + u'\frac{\partial u'}{\partial x'} + w'\frac{\partial u'}{\partial y'}\right] = -\frac{\partial p'}{\partial x'} + \frac{\partial \tau'_{x'x'}}{\partial x'} + \frac{\partial \tau'_{x'y'}}{\partial y'} + \rho g\ sin\alpha, \tag{2}$$

$$\rho\left[\frac{\partial w'}{\partial t'} + u'\frac{\partial w'}{\partial x'} + w'\frac{\partial w'}{\partial y'}\right] = -\frac{\partial p'}{\partial y'} + \frac{\partial \tau'_{x'y'}}{\partial x'} + \frac{\partial \tau'_{y'y'}}{\partial y'} + \rho g\ cos\alpha, \tag{3}$$

$$\rho C_p\left[\frac{\partial T'}{\partial t'} + u'\frac{\partial T'}{\partial x'} + w'\frac{\partial w'}{\partial y'}\right] = \tau'_{x'y'}\left(\frac{\partial u'}{\partial x'} + \frac{\partial w'}{\partial y'}\right) + k_1\left[\frac{\partial}{\partial x'}\left(k(T')\frac{\partial T'}{\partial x'}\right) + \frac{\partial}{\partial y'}\left(k(T')\frac{\partial T'}{\partial y'}\right)\right] + \tau'_{x'x'}\frac{\partial u'}{\partial x'} + \tau'_{y'y'}\frac{\partial w'}{\partial y'}, \tag{4}$$

$$\left[\frac{\partial C'}{\partial t'} + u'\frac{\partial C'}{\partial x'} + w'\frac{\partial C'}{\partial y'}\right] = \frac{DK_T}{T_m}\left[\frac{\partial^2 T'}{\partial (x')^2} + \frac{\partial^2 T'}{\partial (y')^2}\right] + D\left[\frac{\partial^2 C'}{\partial (x')^2} + \frac{\partial^2 C'}{\partial (y')^2}\right], \tag{5}$$

where u', w' are velocity components in radial and axial directions respectively. ρ is the fluid density, p' is the pressure, $\tau'_{x'x'}$, $\tau'_{x'y'}$, $\tau'_{y'y'}$ are extra stress components, while k_1, T', C_p denotes mass diffusivity coefficient, temperature and the specific heat at constant volume respectively.

The problem's boundary conditions are as follows:

$$\psi = \frac{F}{2},\ \frac{\partial^2 \psi'}{\partial y'} = 0,\ \frac{\partial T'}{\partial y'} = 0,\ \frac{\partial C'}{\partial y'} = 0 \text{ at } y' = 0, \tag{6}$$

$$\frac{\partial \psi'}{\partial y'} + \beta_1 \tau'_{x'x'} = -c, T' + \beta_2 \frac{\partial T'}{\partial y'} = T', C' + \beta_3 \frac{\partial C'}{\partial y'} = C'$$
$$\text{at } y' = H' = l(x') + bsin\left(\frac{2\pi}{\lambda}(x' - ct')\right), \tag{7}$$

where H' is the non-uniform wave in which $l(x')$ is the non-uniform radius, b' is the wave amplitude, λ is the wavelength, c is the wave propagation speed and t' is the time. Introducing the dimensionless quantities:

$$x = \frac{x'}{\lambda}, y = \frac{y'}{a}, w = \frac{w'}{c}, u = \frac{\lambda u'}{ca}, t = \frac{ct'}{\lambda}, \tau_{xx} = \frac{a\tau'_{x'x'}}{c\mu_0},$$
$$\tau_{xy} = \frac{a\tau'_{x'y'}}{c\mu'_0}, \tau_{yy} = \frac{a\tau'_{y'y'}}{c\mu_0}, \delta = \frac{a}{\lambda}, p = \frac{a^2 p'}{c\lambda\mu_0}, Re = \frac{ac\rho}{\mu_0},$$
$$\theta = \frac{T' - T'_0}{T_1 - T_0}, F = \frac{\nu c}{ga'^2}, \mu'_0 = \frac{\mu_0}{\mu}, \psi = \frac{\psi'}{ac}, E_1 = \frac{-\tau a^3}{\lambda^3\mu_0 c},$$
$$E_2 = \frac{ma^3 c}{\lambda^3\mu_0}, E_3 = \frac{ca^3}{\lambda^3\mu_0}, E_4 = \frac{ma^3}{\lambda^5\mu_0 c}, E_5 = \frac{Ha^3}{\lambda\mu_0 c},$$
$$Ec = \frac{c^2}{\delta T_0}, Pr = \frac{\mu C_p}{k_1}, Br = PrEc, \nu = \frac{\mu_0}{\rho}, \epsilon = \frac{b}{a},$$
$$h = \frac{H'}{a} = 1 + mx + \epsilon sin(2\pi(x - t)), \tag{8}$$

$$\mu(y) = 1 - \alpha_1 y, \qquad k(\theta) = 1 + \alpha_2 \theta,$$

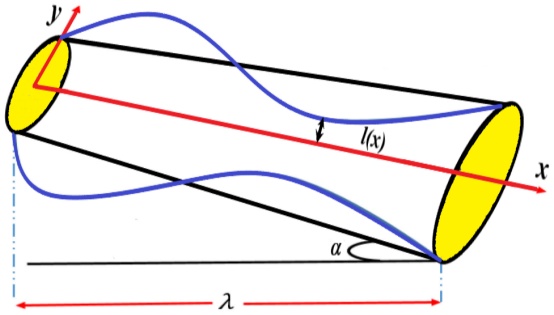

Fig. 1: Geometry of the physical model.

Using equation (8) in equations (1-7) and by using the small Reynolds number and large wavelength approximations, we obtain the non-dimensional governing equations of the form:

$$\frac{\partial p}{\partial x} = \frac{\partial \tau_{xy}}{\partial y} + \frac{sin\alpha}{F}, \tag{9}$$

$$\frac{\partial p}{\partial y} = 0, \tag{10}$$

$$\frac{\partial}{\partial y}\left(k(\theta)\frac{\partial \theta}{\partial y}\right) + Br\tau_{xy}\frac{\partial^2 \psi}{\partial y^2} = 0, \tag{11}$$

$$\frac{\partial^2 \phi}{\partial y^2} + ScSr\frac{\partial^2 \theta}{\partial y^2} = 0, \tag{12}$$

where Br is Brinkman number and τ_{xy} is the constitutive equation of Eyring Powell fluid given as

$$\tau_{xy} = (\mu(y) + B)\frac{\partial^2 \psi}{\partial y^2} - \frac{A}{3}\left(\frac{\partial^2 \psi}{\partial y^2}\right)^3, \tag{13}$$

The non-dimensional boundary conditions are denoted by

$$\psi = \frac{F}{2},\ \frac{\partial^2 \psi}{\partial y^2} = 0,\ \frac{\partial \theta}{\partial y} = 0, \frac{\partial \phi}{\partial y} = 0 \text{ at } y = 0, \tag{14}$$

$$\frac{\partial \psi}{\partial y} + \beta_1 \tau_{xx} = -1,\quad \theta + \beta_2 \frac{\partial \theta}{\partial y} = 1,\quad \phi + \beta_3 \frac{\partial \phi}{\partial y} = 1$$
$$\text{at } y = h = 1 + mx + \epsilon sin(2\pi(x - t)), \tag{15}$$

where β_1, β_2, and β_3 are slip parameters for velocity, temperature, and concentration respectively.

The viscosity varies across the thickness of the channel wall is given by $\mu(y) = 1 - \alpha_1 y$, for $\alpha_1 << 1$, where α_1 is the coefficient of variable viscosity.

The varying thermal conductivity with temperature is defined as $k(\theta) = 1 + \alpha_2\theta$, for $\alpha_2 << 1$, where α_2 is the coefficient of variable thermal conductivity.

III. Solution Methodology

The equations (9) and (11) are nonlinear in nature. Consider equation (9). Let $P = \frac{\partial p}{\partial x}$ and $f = \frac{sin\alpha}{F}$. On integrating equation (9), we get

$$\tau = (P - f)y, \tag{16}$$

Substituting equation (13) in the above equation, we obtain a nonlinear equation. Similarly, on integrating equation (11), a nonlinear equation is obtained. As the analytical solution for nonlinear expression is tedious, the series solution using the perturbation technique is introduced.

Perturbation technique:

To solve the streamline function and temperature expression, the series perturbation technique is applied by using the equations below:

$$\psi = \Sigma A^n \psi_n, \tag{17}$$
$$\theta = \Sigma A^n \theta_n, \tag{18}$$

Ignoring terms of order A^2 and above in equation (17), we obtain a streamline function as

$$\psi = \psi_0 + A\psi_1, \tag{19}$$

The zeroth order streamline equation with boundary conditions is given by

$$\begin{aligned}&(P-f)y = (1-\alpha_1 y+B)\frac{\partial^2\psi_0}{\partial y^2},\\ &\psi_0 = \frac{F}{2}, \quad \frac{\partial^2\psi_0}{\partial y^2} = 0 \ \text{ at } \ y=0 \quad \text{and}\\ &\frac{\partial\psi_0}{\partial y} + \beta_1(1-\alpha_1 y+B)\frac{\partial^2\psi_0}{\partial y^2} = -1 \ \text{ at } \ y=h,\end{aligned} \tag{20}$$

The first order streamline equation with boundary conditions is given by

$$\begin{aligned}&(1-\alpha_1 y+B)\frac{\partial^2\psi_1}{\partial y^2} - \frac{1}{3}(\frac{\partial^2\psi_0}{\partial y^2})^3 = 0,\\ &\psi_1 = 0, \quad \frac{\partial^2\psi_1}{\partial y^2} = 0 \ \text{ at } \ y=0 \quad \text{and}\\ &\frac{\partial\psi_1}{\partial y} + \beta_1\left((1-\alpha_1 y+B)\frac{\partial^2\psi_0}{\partial y^2} - \frac{1}{3}\left(\frac{\partial^2\psi_0}{\partial y^2}\right)^3\right) = 0\\ &\text{at } \ y=h,\end{aligned} \tag{21}$$

Similarly, by ignoring A^2 and above terms in equation (18), we obtain temperature expression as,

$$\theta = \theta_0 + A\theta_1, \tag{22}$$

The zeroth order temperature equation with boundary conditions is given by

$$\begin{aligned}&\frac{\partial\theta_0}{\partial y} + \alpha_2\theta_0\frac{\partial\theta_0}{\partial y} + D_1 = 0,\\ &\frac{\partial\theta_0}{\partial y} = 0 \ \text{ at } \ y=0 \ \text{ and}\\ &\theta_0 + \beta_2\frac{\partial\theta_0}{\partial y} = 1 \ \text{ at } \ y=h,\end{aligned} \tag{23}$$

The first order temperature equation with boundary conditions is given by

$$\begin{aligned}&\frac{\partial\theta_1}{\partial y} + \alpha_2\theta_0\frac{\partial\theta_1}{\partial y} + \alpha_2\theta_1\frac{\partial\theta_0}{\partial y} + D_2 = 0,\\ &\frac{\partial\theta_1}{\partial y} = 0 \ \text{ at } \ y=0 \quad \text{and}\\ &\theta_1 + \beta_2\frac{\partial\theta_1}{\partial y} = 0 \ \text{ at } \ y=h,\end{aligned} \tag{24}$$

The equations (20), (21), (23), and (24) are nonlinear; hence we apply double perturbation technique to obtain the series solution for streamline and temperature equation as follows.

$$\psi_i = \Sigma\alpha_1^j\psi_{ij} \ \text{ where } \ 0\le i\le n, \ \ 0\le j\le n, \tag{25}$$
$$\theta_i = \Sigma\alpha_2^j\theta_{ij} \ \text{ where } \ 0\le i\le n, \ \ 0\le j\le n, \tag{26}$$

Ignoring higher order terms, like $O(\alpha_1^2)$, $O(\alpha_2^2)$ and above, the final expressions for streamlines, and temperature are obtained as follows.
The streamline equations obtained from equation (25) are,

$$\psi_0 = \psi_{00} + \alpha_1\psi_{01}, \tag{27}$$
$$\psi_1 = \psi_{10} + \alpha_1\psi_{11}, \tag{28}$$

Substituting equations (27) and (28) in equation (19), the expression for streamline is obtained as,

$$\psi = \psi_{00} + \alpha_1\psi_{01} + A\psi_{10} + A\alpha_1\psi_{11}, \tag{29}$$

where

$$\begin{aligned}\psi_{00} &= \frac{My^3}{6(1+B)} + y\left(-1 - \frac{Mh^2}{2(1+B)} - \eta_1 Mh\right) + \frac{F}{2}\\ \psi_{01} &= \left(\frac{My^4}{12(1+B)^2} - \frac{Mh^3}{3(1+B)^2}y\right)\\ \psi_{10} &= \left(\frac{M^3y^5}{60(1+B)^4} - \frac{M^3h^4}{12(1+B)^4}y\right)\\ \psi_{11} &= \left(\frac{4M^3y^6}{90(1+B)^5} - \frac{4M^3h^5}{15(1+B)^5}y\right)\end{aligned}$$

Similarly, the following temperature expression is obtained by using equation (26),

$$\theta_0 = \theta_{00} + \alpha_2\theta_{01}, \tag{30}$$
$$\theta_1 = \theta_{10} + \alpha_2\theta_{11}, \tag{31}$$

Substituting equations (30) and (31) in equation (22), the expression for temperature is obtained as,

$$\theta = \theta_{00} + \alpha_2\theta_{01} + A\theta_{10} + A\alpha_2\theta_{11}, \tag{32}$$

where

$$\begin{aligned}\theta_{00} &= 1 + A_1 - A_2 + \beta_2 A_3\\ \theta_{01} &= A_5 - A_6 + A_7 - A_8 + A_9 - A_{10} + A_2A_4 - A_1A_4\\ &\quad + A_{11} - A_{12} + \beta_2(A_{13} + A_{14} + A_{15} + A_{16} + A_3A_4)\\ \theta_{10} &= A_{17} - A_{18} + \beta_2 A_{19}\\ \theta_{11} &= -(A_1 + A_4)(A_{17} + A_{20}) + (A_2 + A_4)(A_{18} + A_{20})\\ &\quad + \beta_2(A_{19}A_2 + A_{18}A_3 + A_{20}A_3 + A_{19}A_4)\end{aligned}$$

The analytical solution for velocity is obtained by using the relation,

$$\begin{aligned}&u = \frac{\partial\psi}{\partial y}\\ &u = \frac{M(y^2-h^2)}{2(1+B)} - \eta_1 Mh - 1 + \alpha\frac{M(y^3-h^3)}{3(1+B)^2}\\ &\qquad + A\frac{M^3(y^4-h^4)}{12(1+B)^4} + A\alpha\frac{4M^3(y^5-h^5)}{15(1+B)^5}\end{aligned} \tag{33}$$

where

$$\begin{aligned}&M = P - f,\\ &P = E_1\frac{\partial^3 h}{\partial x^3} + E_2\frac{\partial^3 h}{\partial t^2\partial x} + E_3\frac{\partial^2 h}{\partial t\partial x} + E_4\frac{\partial^5 h}{\partial x^5} + E_5\frac{\partial h}{\partial x}\end{aligned}$$

The analytical solution for concentration is obtained by solving the equation (12). The solution is given as follows,

$$\begin{aligned}\phi =& 1 - ScSr[G_1 + AG_2 + \alpha_2(A_4G_1 + G_3) + A\alpha_2A_{20}G_1\\ &+ A\alpha_2(A_4G_2 + G_4)] + ScSr[G_5 + \alpha_2(A_4G_5 + G_7)\\ &+ \alpha_2(A_{20}G_5 + A_4G_6 + G_8)] + \beta_3 ScSr[G_9 + AG_{10}\\ &+ \alpha_2(A_4G_9 + G_{11}) + \alpha_2(A_{20}G_9 + A_4G_{10} + G_{12})]\end{aligned} \tag{34}$$

IV. Results and Discussions

In this section, the pre-eminent objective is to interpret the influence of material parameters, slip conditions, variable liquid properties, inclination angle, non-uniform parameters, and wall properties on velocity, temperature, concentration, and streamlines have been discussed. MATLAB 2022a programming is used to calculate the impact of the above parameter with the help of graphs.

A. Velocity Profiles

Fig.2 and Fig.3 depicts the variation of fitting parameters of velocity profiles. Fig.2(a) shows that axial velocity increases with an increase in the Eyring Powell parameter A, while in Fig.2(b), the opposite behaviour is seen for the material parameter B. Fig.2(c)-(d) shows an enhancement in the velocity profile for variable viscosity and velocity slip parameters which indicates that variable viscosity coefficient and velocity slip parameter are indispensable in observing the velocity profile. The velocity profile has an increasing behaviour when the angle of inclination increases, as shown in Fig.2(e), and has a similar effect to the rise in non-uniform parameter (see Fig.2(f)). Fig.3(a) depicts the variation of velocity profiles for variation in amplitude ratio. As the amplitude ratio increases, the velocity also improves. In Fig.3(b), increasing variation in wall tension and mass characterisation parameters increases the velocity in the axial direction. The increase in the wall-damping parameter has the opposite effect on the velocity profiles. A similar effect is seen in the case of wall rigidity and wall elasticity parameter. The velocity profiles is a decreasing function for increasing wall rigidity parameters and increasing wall elasticity parameter.

B. Temperature Profiles

Fig.4 and Fig.5 illustrates the variation of parameters of temperature profiles. Fig.4(a) shows that the temperature increases with an increase in the Eyring Powell parameter A, while in Fig.4(b), the opposite behaviour is observed for the material parameter B. Fig.4(c)-(d) shows a negligible increase in the temperature profile for variable viscosity while increasing variable thermal conductivity decreases the temperature profiles. The graph indicates that the variable viscosity coefficient has not much effect on the temperature of the fluid. Still, the varying thermal conductivity parameter is vital in observing the temperature profiles. It is noticed that the fluid temperature rises when the angle of inclination increases as seen in Fig.5(a) and has a similar effect to the rise in non-uniform parameter (see Fig.5(b)). Fig.5(c) has been drawn to analyse the effect of thermal slip over the temperature. It shows that the increase in temperature as the thermal slip parameter increases. A considerable enhancement in the temperature can be observed in the case of an increase in Brinkman number (see Fig.5(d)). Fig.5(e) shows that a higher amplitude ratio enhances the temperature profiles. Fig.5(f) shows that an increasing variation in wall tension and mass characterisation parameters increases the temperature in the axial direction. The increase in the wall-damping parameter has the opposite effect on the temperature profiles. A similar behaviour is seen in the case of wall rigidity and wall elasticity parameters. The temperature profile decreases due to the increase in wall rigidity parameter and wall elasticity parameter.

C. Concentration Profiles

This subsection explains the effects of pertinent parameters over the concentration, which are represented graphically in Fig. 6 and Fig.7. Fig.6(a) shows that the concentration profile decreases with an increase in the Eyring Powell parameter A. At the same time, the opposite behaviour is observed for the material parameter B (see Fig.6(b)). Fig.6(c) shows that increasing variable thermal conductivity diminishes the concentration profiles. Fig.6(d) shows the rise in concentration with a decrease in the thermal slip parameter. A similar outcome is seen in Fig.6(e). i.e., as the concentration slip parameter increases, a reduction in the concentration profiles can be observed. There is a noticeable decrease in the concentration profile when the inclination angle increases in Fig.6(f). A significant change in the concentration can be observed in case of the Brinkman number, as shown in Fig.7(a). The concentration profile decreases with an increase in Brinkman number. Similar behaviour is noticed in the case of Schmidt number, and Soret number. Increasing these values reduces the concentration profiles, as seen in Fig.7(b) and Fig.7(c) respectively. In Fig.7(d), while increase in wall tension and mass characterisation parameters decrease the concentration of the fluid particles in the axial direction, increase in the wall-damping parameter has the opposite impact on the concentration profiles. A similar effect is seen in the case of wall rigidity and wall elasticity parameter. The concentration profile increases due to the increase in wall rigidity parameter and wall elasticity parameter.

D. Trapping phenomenon

The most important phenomena in the peristalsis is Trapping. This phenomena occurs during the peristalsis when few of its streamlines gets closed resulting in the formulation of boluses which circulates internally and move forward with the speed of the peristaltic wave. These streamlines are represented in Fig.8-12. Fig.8 illustrates the variation in streamlines for various values of fluid parameter A. The bolus has grown in size for an increment in A. Fluid parameter B exhibits the opposite tendency in Fig.9 as a rise in from B reduces the number of boluses. The streamlines for changing the coefficient of variable viscosity are shown in Fig.10. The bolus size grows as variable viscosity does. Fig.11 depicts the variation for the velocity slip parameter. The number of boluses increases for an increase in the velocity slip parameter. Fig.12 shows the effect of several wall characteristics in the formation of bolus. Fig.12(a) represents effect of different wall parameters for specific values. The size of the bolus grows as the wall tension parameter rises, as shown in Fig.12(b). As the mass characteristic parameter increases, the number of formation of boluses also increases (see Fig.12(b) and Fig.12(c)). However, in Fig.12(d), the bolus size shrinks as the wall-damping parameter value rises. A similar trend is seen in Fig.12(e), where the greater value of wall rigidity results in fewer trapped boluses. The size of the bolus formed has been significantly reduced for an increase in the wall elasticity parameter. (see Fig.12(f)). This shows that wall characteristics plays an important role in the formation of the bolus.

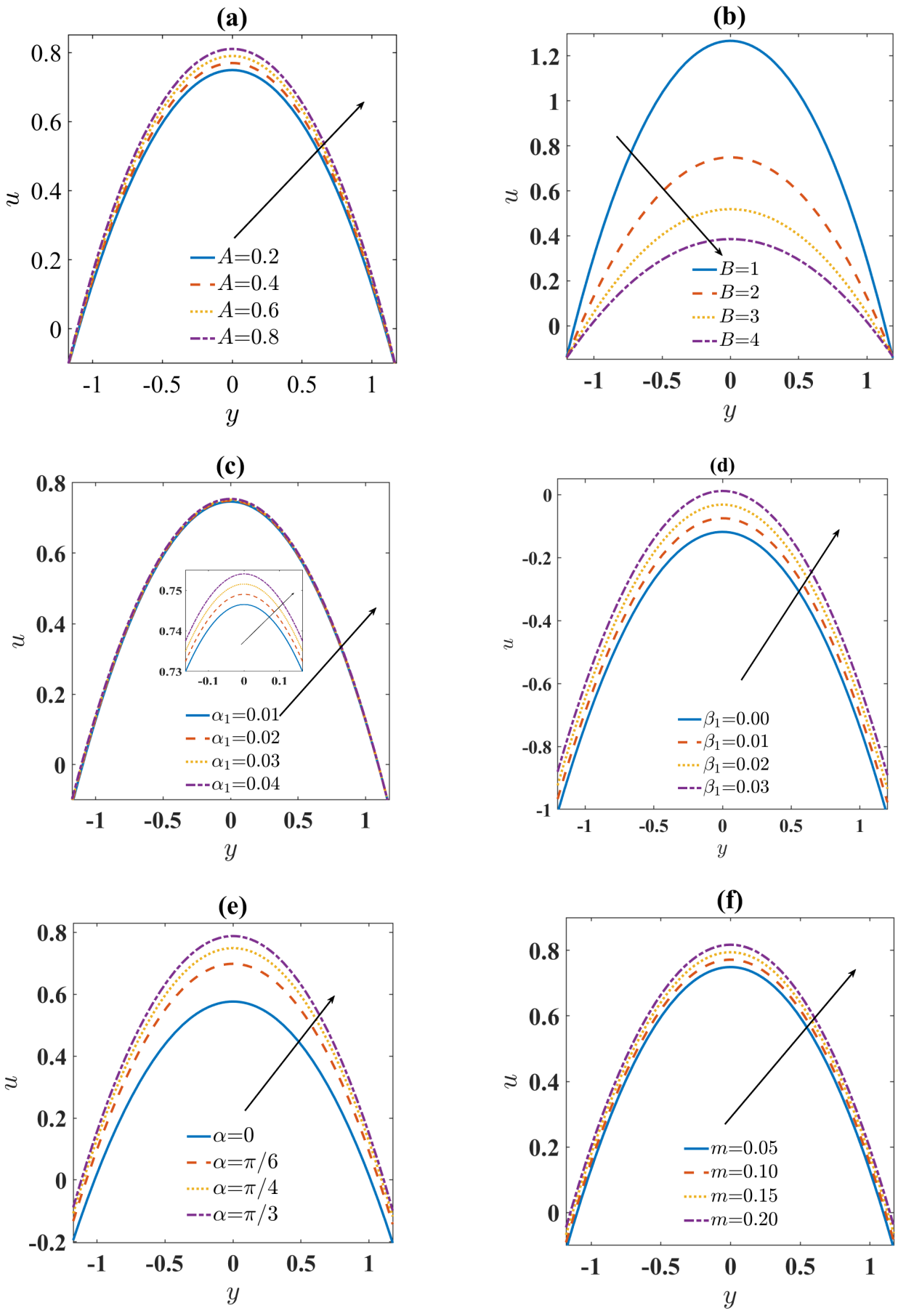

Fig. 2: Variation of velocity profiles when $E_1 = 0.1, E_2 = 0.04, E_3 = 0.045, E_4 = 0.002, E_5 = 0.04, A = 0.2, B = 2, x = 0.2, F = 2, t = 0.1, \alpha = \frac{\pi}{4}, \alpha_1 = 0.02, \beta_1 = 0.02, \epsilon = 0.3, m = 0.05$.

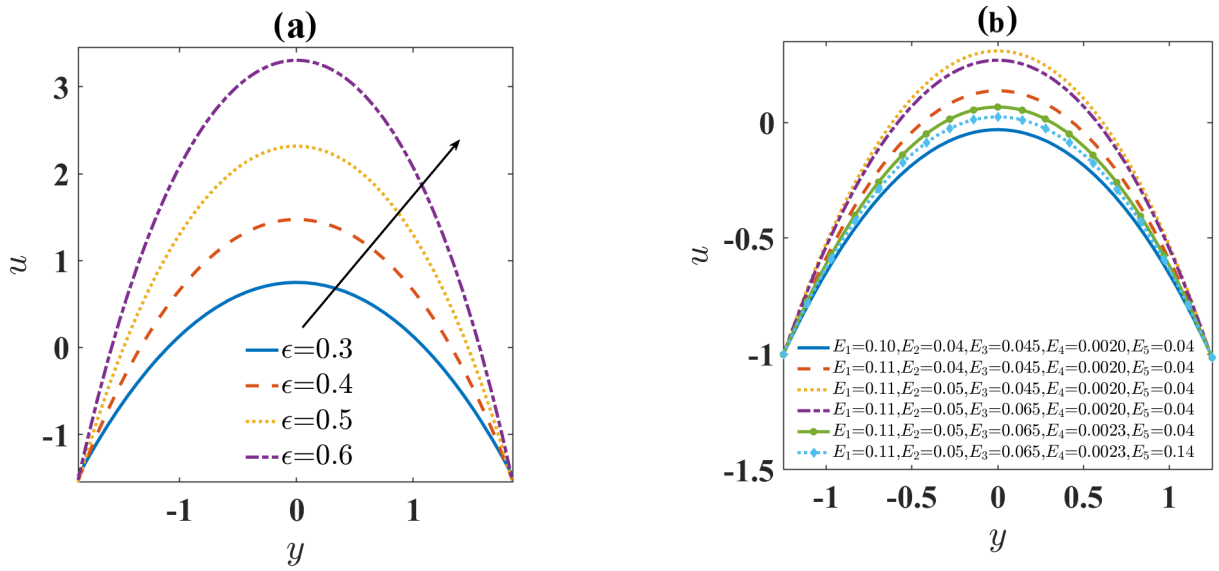

Fig. 3: Variation of velocity profiles when $E_1 = 0.1, E_2 = 0.04, E_3 = 0.045, E_4 = 0.002, E_5 = 0.04, A = 0.2, B = 2, x = 0.2, F = 2, t = 0.1, \alpha = \frac{\pi}{4}, \alpha_1 = 0.02, \beta_1 = 0.02, \epsilon = 0.3, m = 0.05$.

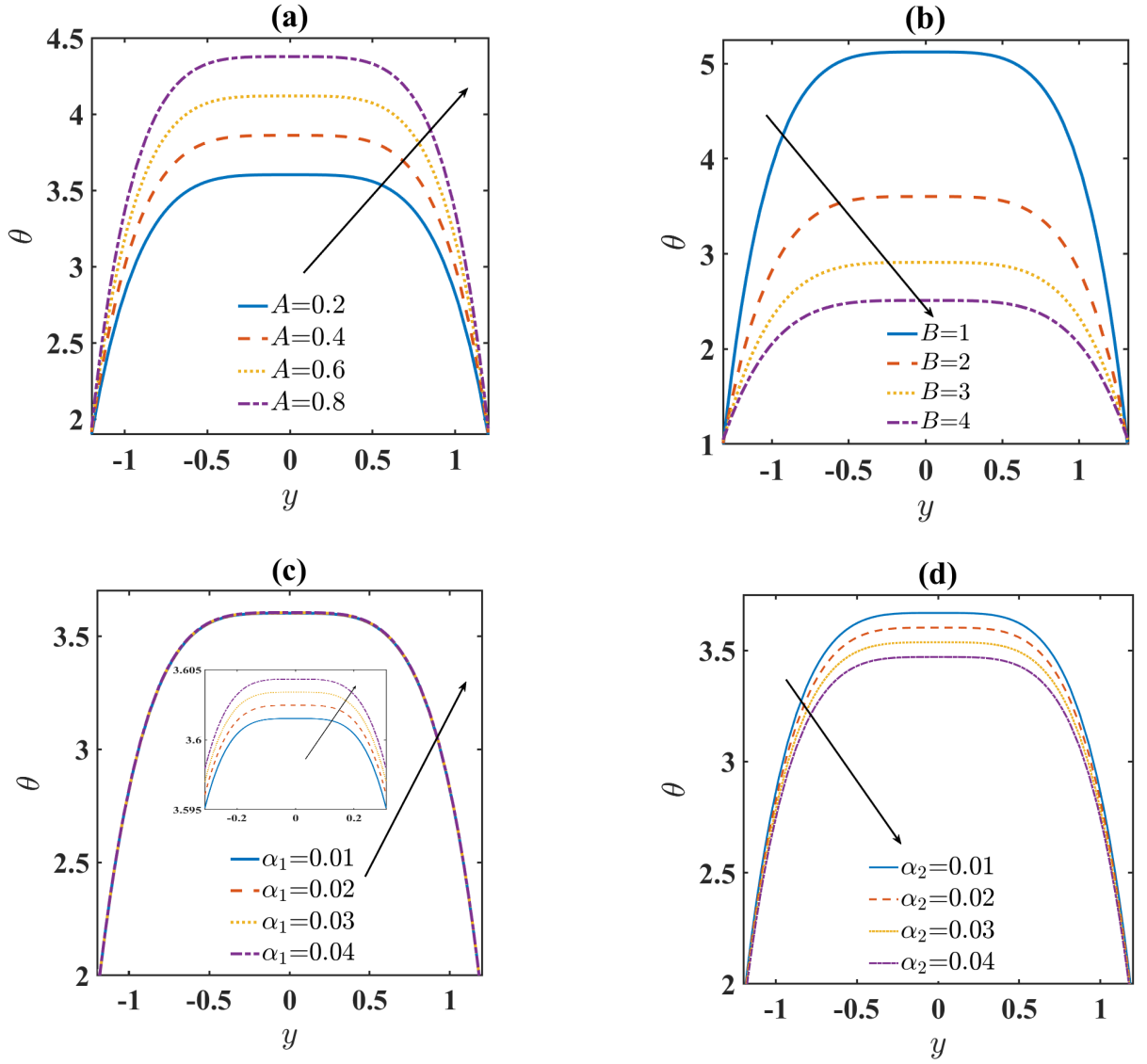

Fig. 4: Variation of temperature profiles when $E_1 = 0.1, E_2 = 0.04, E_3 = 0.045, E_4 = 0.002, E_5 = 0.04, A = 0.2, B = 2, x = 0.2, F = 2, t = 0.1, \alpha = \frac{\pi}{4}, Br = 1, \alpha_1 = 0.02, \alpha_2 = 0.02, \beta_2 = 0.02, \epsilon = 0.3, m = 0.05$.

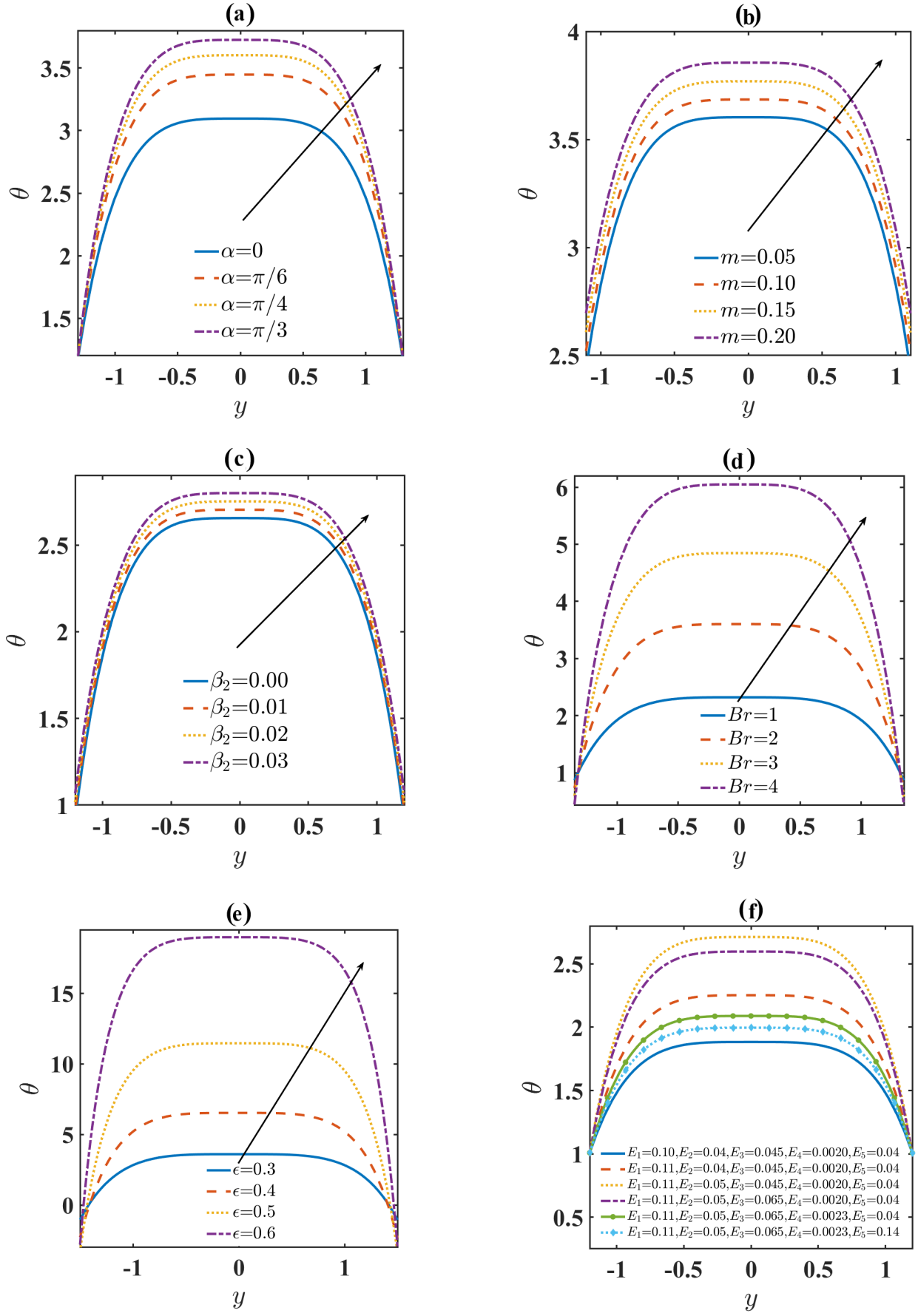

Fig. 5: Variation of temperature profiles when $E_1 = 0.1, E_2 = 0.04, E_3 = 0.045, E_4 = 0.002, E_5 = 0.04, A = 0.2, B = 2, x = 0.2, F = 2, t = 0.1, \alpha = \frac{\pi}{4}, Br = 1, \alpha_1 = 0.02, \alpha_2 = 0.02, \beta_2 = 0.02, \epsilon = 0.3, m = 0.05$.

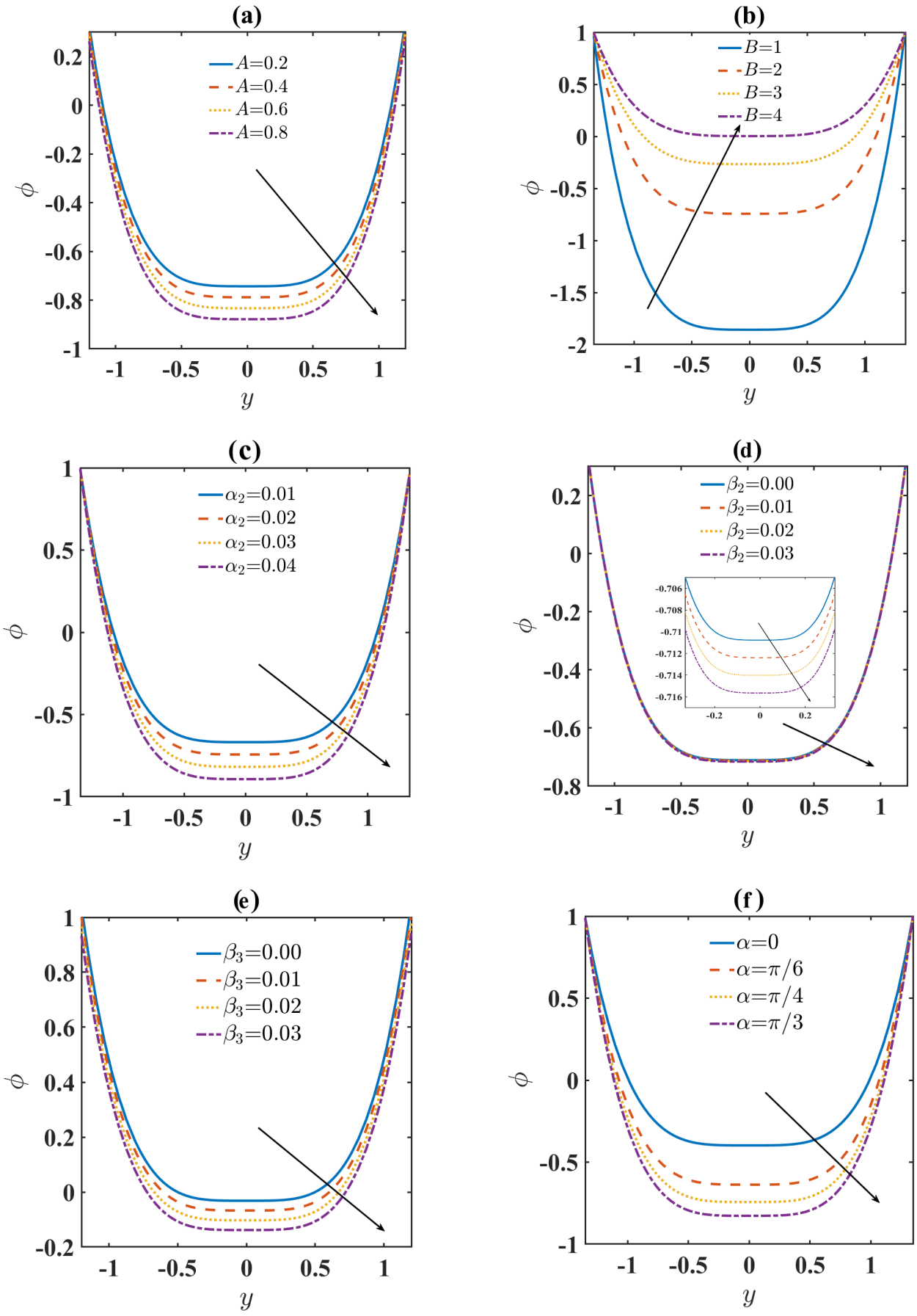

Fig. 6: Variation of concentration profiles when $E_1 = 0.1, E_2 = 0.04, E_3 = 0.045, E_4 = 0.002, E_5 = 0.04, A = 0.2, B = 2, x = 0.2, F = 2, t = 0.1, \alpha = \frac{\pi}{4}, Br = 1, Sc = 1, Sr = 1, \alpha_1 = 0.02, \alpha_2 = 0.02, \beta_2 = 0.02, \beta_3 = 0.02, \epsilon = 0.3, m = 0.05$.

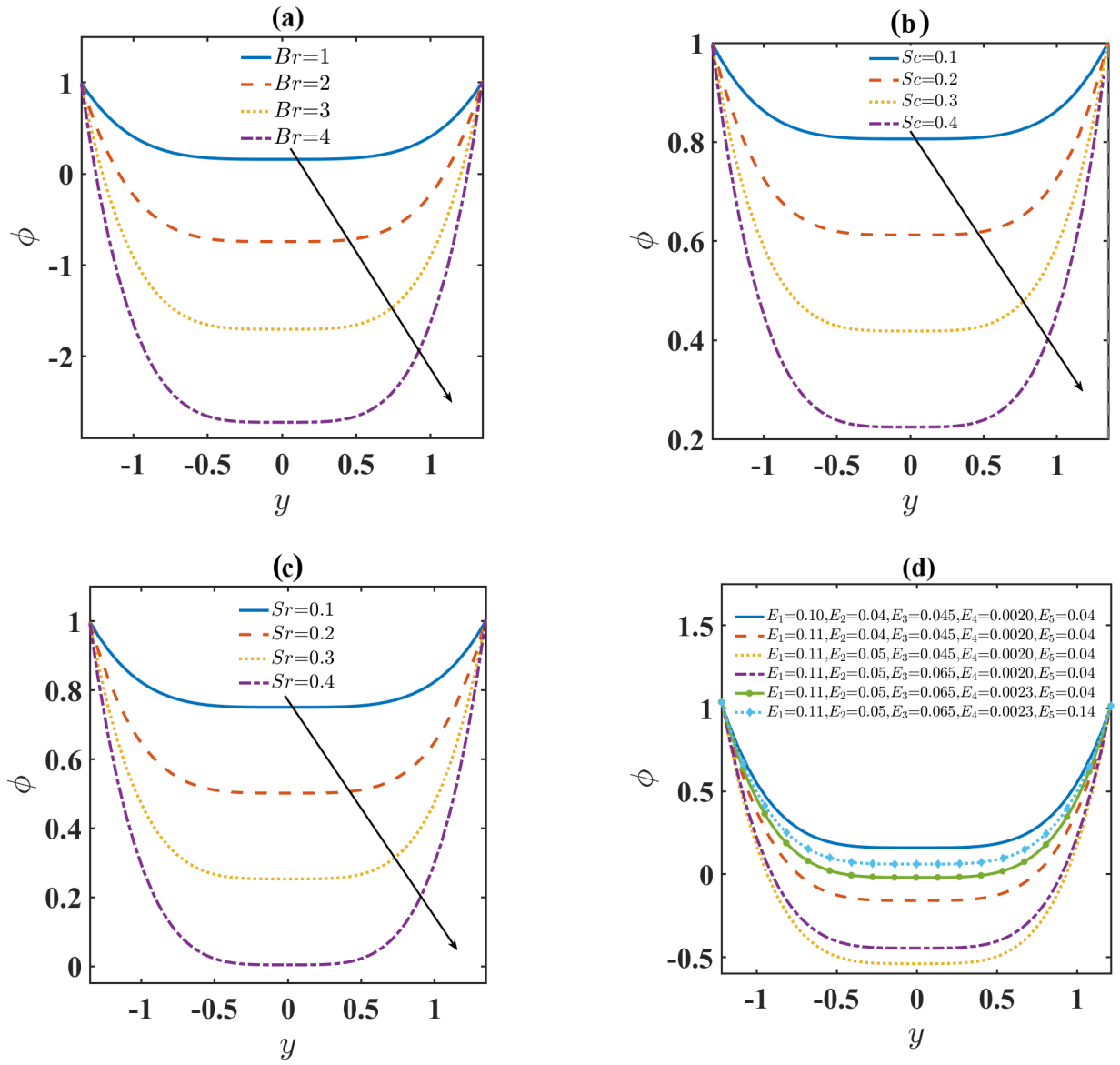

Fig. 7: Variation of concentration profiles when $E_1 = 0.1, E_2 = 0.04, E_3 = 0.045, E_4 = 0.002, E_5 = 0.04, A = 0.2, B = 2, x = 0.2, F = 2, t = 0.1, \alpha = \frac{\pi}{4}, Br = 1, Sc = 1, Sr = 1, \alpha_1 = 0.02, \alpha_2 = 0.02, \beta_2 = 0.02, \beta_3 = 0.02, \epsilon = 0.3, m = 0.05$.

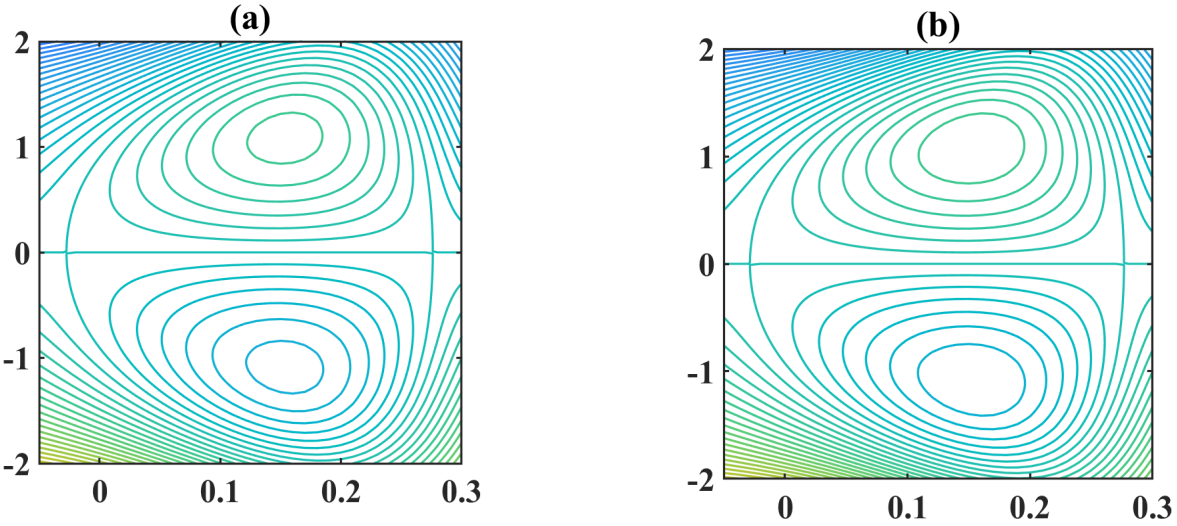

Fig. 8: Variation of streamlines for (a) $A = 0.2$ (b) $A = 0.4$

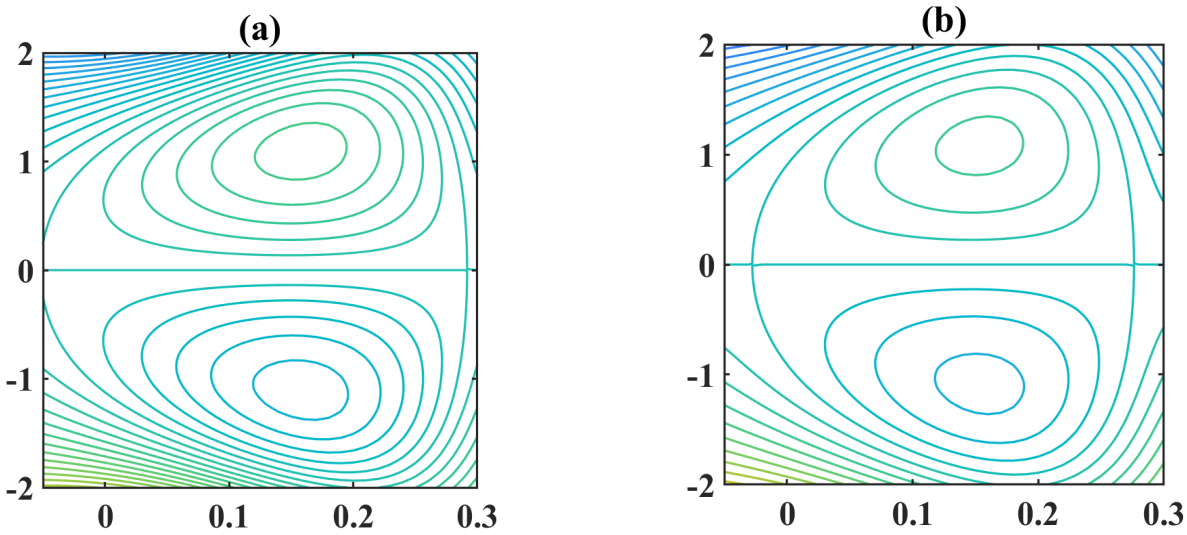

Fig. 9: Variation of streamlines for (a) $B = 1.8$ (b) $B = 2.2$

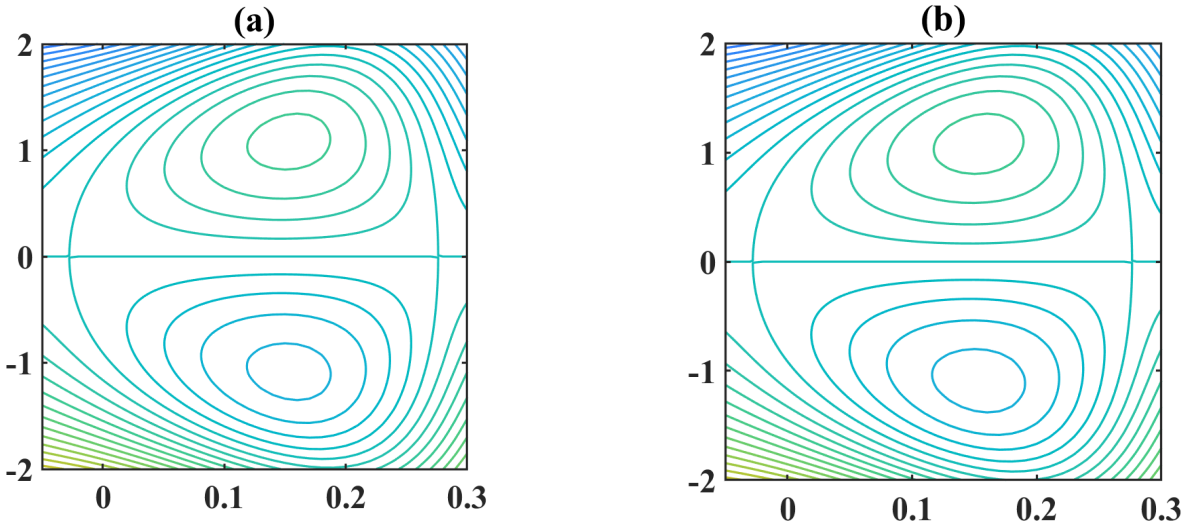

Fig. 10: Variation of streamlines for (a) $\alpha_1 = 0.01$ (b) $\alpha_1 = 0.04$

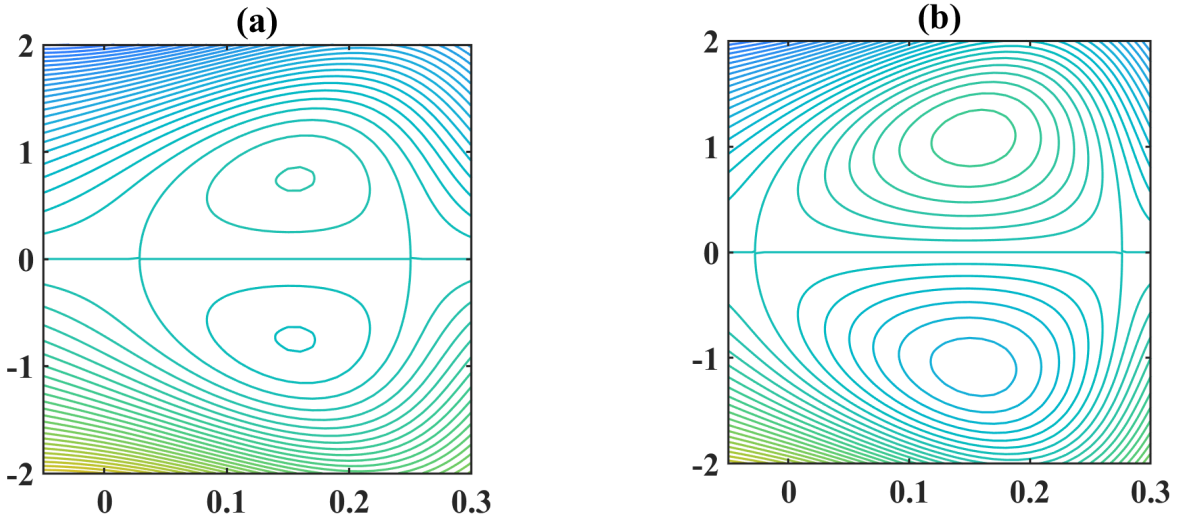

Fig. 11: Variation of streamlines for (a) $\beta_1 = 0.00$ (b) $\beta_1 = 0.03$

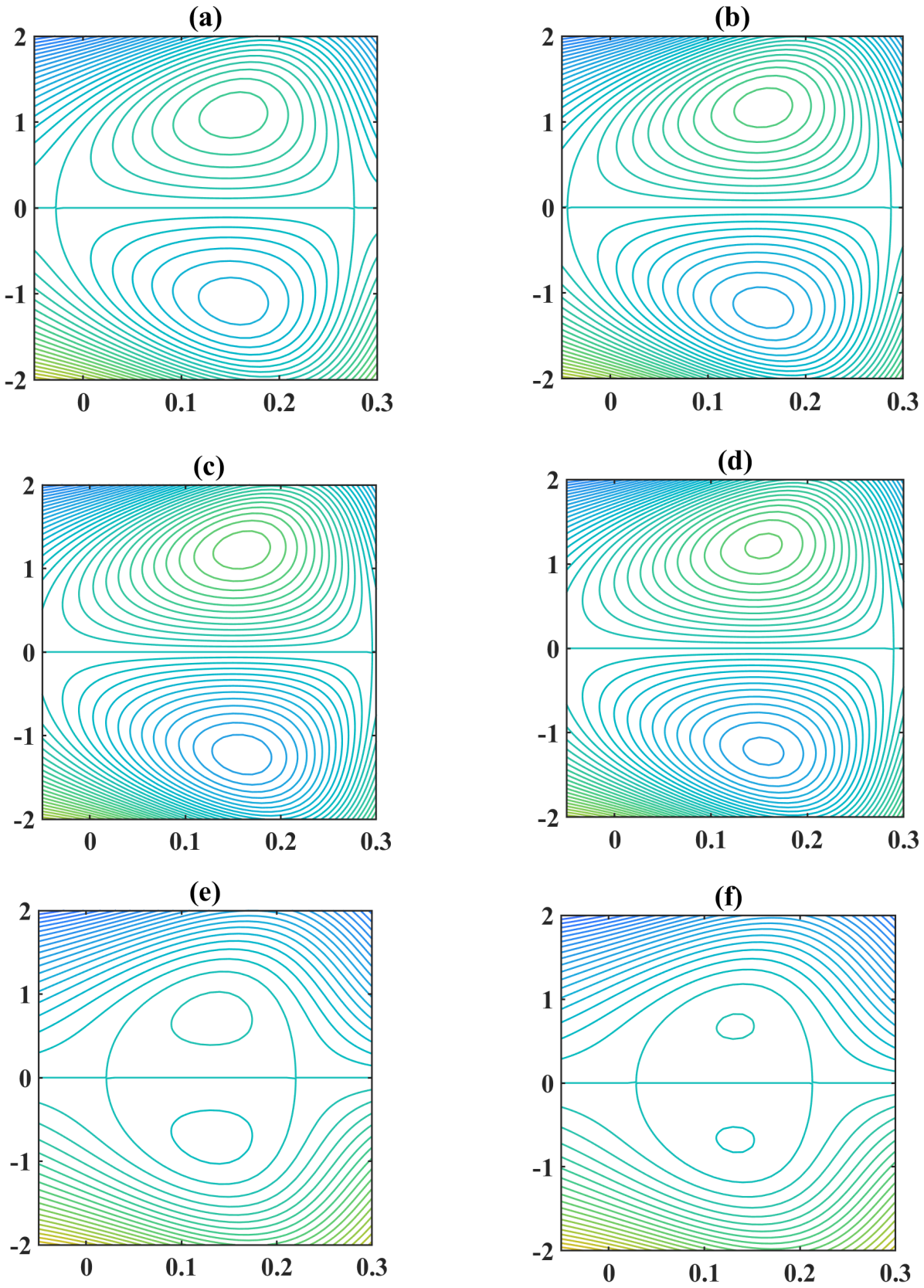

Fig. 12: Variation of streamlines for (a) $E_1 = 0.1, E_2 = 0.04, E_3 = 0.045, E_4 = 0.002, E_5 = 0.04$ (b) $E_1 = 0.11, E_2 = 0.04, E_3 = 0.045, E_4 = 0.002, E_5 = 0.04$ (c) $E_1 = 0.11, E_2 = 0.05, E_3 = 0.045, E_4 = 0.002, E_5 = 0.04$ (d) $E_1 = 0.11, E_2 = 0.05, E_3 = 0.065, E_4 = 0.002, E_5 = 0.04$ (e) $E_1 = 0.11, E_2 = 0.05, E_3 = 0.065, E_4 = 0.003, E_5 = 0.04$ (f) $E_1 = 0.11, E_2 = 0.05, E_3 = 0.065, E_4 = 0.003, E_5 = 0.10$

V. Conclusion

A non-uniform channel is considered in our initial investigation to examine the peristaltic flow of an Eyring Powell fluid while taking slip, variable viscosity, and variable thermal conductivity into account. The current study explains the movement of chyme into the gastrointestinal system and blood flows through small arteries, where fluid viscosity changes depending on wall thickness. Following are the preliminary results from the current model:

- Eyring Powell fluid parameters show opposite behaviour for velocity, temperature, and concentration profiles.
- The variable viscosity enhance both temperature and velocity profiles.
- The temperature profiles are improved by increasing Brinkman number, whereas the concentration profiles exhibit opposite behaviour.
- Variable thermal conductivity decreases both temperature and concentration profiles.
- Velocity slip parameters improves the number of trapped boluses.

Appendix

$$D_1 = \frac{Br(P-f)^2}{(1+B)}\left[\frac{y^3}{3}+\frac{\alpha_1 y^4}{2(1+B)}+\frac{\alpha_1^2 y^5}{5(1+B)^2}\right] - \frac{Br\alpha_1(P-f)^2}{(1+B)}\left[\frac{y^4}{4}+\frac{2\alpha_1 y^5}{5(1+B)}+\frac{\alpha_1^2 y^6}{6(1+B)^2}\right]$$

$$D_2 = \frac{Br(P-f)^4}{(1+B)^4}\left[\frac{y^5}{15}+\frac{4\alpha_1 y^6}{18(1+B)}-\frac{8\alpha_1^2 y^7}{21(1+B)^2}\right] + Br(P-f)^4\left[-\frac{12\alpha_1^3 y^8}{24(1+B)^7}-\frac{8\alpha_1^4 y^9}{27(1+B)^8}\right]$$

$$A_1 = \frac{Br(P-f)^2}{(1+B)}\left[\frac{y^4}{12}+\frac{2\alpha_1 y^5}{20(1+B)}+\frac{\alpha_1^2 y^6}{30(1+B)^2}\right] - \frac{Br\alpha_1(P-f)^2}{(1+B)}\left[\frac{y^5}{20}+\frac{2\alpha_1 y^6}{30(1+B)}+\frac{\alpha_1^2 y^7}{42(1+B)^2}\right]$$

$$A_2 = \frac{Br(P-f)^2}{(1+B)}\left[\frac{h^4}{12}+\frac{2\alpha_1 h^5}{20(1+B)}+\frac{\alpha_1^2 h^6}{30(1+B)^2}\right] - \frac{Br\alpha_1(P-f)^2}{(1+B)}\left[\frac{h^5}{20}+\frac{2\alpha_1 h^6}{30(1+B)}+\frac{\alpha_1^2 h^7}{42(1+B)^2}\right]$$

$$A_3 = \frac{Br(P-f)^2}{(1+B)}\left[\frac{h^3}{3}+\frac{\alpha_1 h^4}{2(1+B)}+\frac{\alpha_1^2 h^5}{5(1+B)^2}\right] - \frac{Br\alpha_1(P-f)^2}{(1+B)}\left[\frac{h^4}{4}+\frac{2\alpha_1 h^5}{5(1+B)}+\frac{\alpha_1^2 h^6}{6(1+B)^2}\right]$$

$$A_4 = -A_2 + \beta_2 A_3 + 1$$

$$A_5 = -\frac{Br^2(P-f)^4}{(1+B)^2}\left[\frac{y^8}{252}+\frac{17\alpha_1 y^9}{1890(1+B)}\right] - \frac{Br^2(P-f)^4\alpha_1^2 y^{10}}{100(1+B)^4}\left[\frac{3\alpha_1 y}{11(1+B)}+\frac{\alpha_1^2 y^2}{18(1+B)^2}\right] - \frac{7Br^2(P-f)^4\alpha_1^2 y^{10}}{900(1+B)^4}$$

$$A_6 = -\frac{Br^2(P-f)^4}{18(1+B)^2}\left[\frac{h^8}{14}+\frac{17\alpha_1 h^9}{105(1+B)}+\frac{7\alpha_1^2 h^{10}}{50(1+B)^2}\right] - \frac{Br^2(P-f)^4}{(1+B)^5}\left[\frac{3\alpha_1^3 h^{11}}{1100}+\frac{\alpha_1^4 h^{12}}{1800(1+B)}\right]$$

$$A_7 = \frac{Br^2\alpha_1(P-f)^4}{3(1+B)^3}\left[\frac{y^9}{144}+\frac{7\alpha_1 y^{10}}{400(1+B)}\right] + \frac{Br^2\alpha_1^3(P-f)^4}{5(1+B)^5}\left[\frac{14y^{11}}{495}+\frac{\alpha_1 y^{12}}{80(1+B)}\right] + \frac{Br^2\alpha_1^3(P-f)^4}{5(1+B)^5}\frac{\alpha_1^2 y^{13}}{468(1+B)^2}$$

$$A_8 = \frac{Br^2\alpha_1(P-f)^4}{3(1+B)^3}\left[\frac{h^9}{144}+\frac{7\alpha_1 h^{10}}{400(1+B)}\right] + \frac{Br^2\alpha_1^3(P-f)^4}{5(1+B)^5}\left[\frac{14h^{11}}{495}+\frac{\alpha_1 h^{12}}{80(1+B)}\right] + \frac{Br^2\alpha_1^3(P-f)^4}{5(1+B)^5}\frac{\alpha_1^2 h^{13}}{468(1+B)^2}$$

$$A_9 = \frac{Br^2\alpha_1(P-f)^4}{180(1+B)^3}\left[\frac{y^9}{3}+\frac{17\alpha_1 y^{10}}{20(1+B)}+\frac{323\alpha_1^2 y^{11}}{385(1+B)^2}\right] + \frac{Br^2\alpha_1^4(P-f)^4}{(1+B)^6}\left[\frac{157y^{12}}{73800}+\frac{\alpha_1 y^{13}}{2730(1+B)}\right]$$

$$A_{10} = \frac{Br^2\alpha_1(P-f)^4}{180(1+B)^3}\left[\frac{h^9}{3}+\frac{17\alpha_1 h^{10}}{20(1+B)}+\frac{323\alpha_1^2 h^{11}}{385(1+B)^2}\right] + \frac{Br^2\alpha_1^4(P-f)^4}{(1+B)^6}\left[\frac{157h^{12}}{73800}+\frac{\alpha_1 h^{13}}{2730(1+B)}\right]$$

$$A_{11} = -Br^2(P-f)^4\alpha_1^2\left[\frac{y^{10}}{800(1+B)^4}+\frac{\alpha_1 y^{11}}{300(1+B)^5}\right] - \frac{Br^2\alpha_1^3(P-f)^4}{18(1+B)^6}\left[\frac{1011y^{12}}{16400}+\frac{\alpha_1 y^{13}}{35(1+B)}\right] + \frac{Br^2\alpha_1^5(P-f)^4}{3528(1+B)^8}y^{14}$$

$$A_{12} = -Br^2(P-f)^4\alpha_1^2\left[\frac{h^{10}}{800(1+B)^4}+\frac{\alpha_1 h^{11}}{300(1+B)^5}\right] - \frac{Br^2\alpha_1^3(P-f)^4}{18(1+B)^6}\left[\frac{1011h^{12}}{16400}+\frac{\alpha_1 h^{13}}{35(1+B)}\right] + \frac{Br^2\alpha_1^5(P-f)^4}{3528(1+B)^8}h^{14}$$

$$A_{13} = -\frac{Br^2(P-f)^4}{6(1+B)^2}\left[\frac{17\alpha_1 y^8}{35(1+B)}+\frac{7\alpha_1^2 y^9}{150(1+B)^2}\right] - Br^2(P-f)^4\left[\frac{3\alpha_1^3 y^{10}}{100(1+B)^5}+\frac{\alpha_1^4 y^{11}}{150(1+B)^6}\right] - \frac{Br^2(P-f)^4}{36(1+B)^2}y^7$$

$$A_{14} = \frac{Br^2\alpha_1(P-f)^4}{(1+B)^3}\left[\frac{y^8}{48}+\frac{7\alpha_1 y^9}{120(1+B)}\right] + \frac{Br^2\alpha_1^3(P-f)^4}{5(1+B)^5}\left[\frac{14y^{10}}{45}+\frac{3\alpha_1 y^{11}}{20(1+B)}\right] + \frac{Br^2\alpha_1^5(P-f)^4}{180(1+B)^7}y^{12}$$

$$A_{15} = \frac{Br^2\alpha_1(P-f)^4}{60(1+B)^3}\left[y^8 + \frac{17\alpha_1 y^9}{6(1+B)} + \frac{323\alpha_1^2 y^{10}}{105(1+B)^2}\right] + \frac{Br^2\alpha_1(P-f)^4}{30(1+B)^6}\left[\frac{157\alpha_1^3 y^{11}}{205} + \frac{\alpha_1^4 y^{12}}{7(1+B)}\right]$$

$$A_{16} = -Br^2(P-f)^4\alpha_1^2\left[\frac{y^9}{80(1+B)^4} + \frac{11\alpha_1 y^{10}}{300(1+B)^5}\right] - \frac{Br^2\alpha_1^4(P-f)^4}{6(1+B)^6}\left[\frac{13\alpha_1 y^{12}}{105(1+B)} + \frac{\alpha_1^2 y^{13}}{42(1+B)^2}\right] - \frac{Br^2\alpha_1^4(P-f)^4}{(1+B)^6}\frac{1011y^{11}}{24600}$$

$$A_{17} = -\frac{Br(P-f)^4}{(1+B)^4}\left[\frac{y^6}{90} + \frac{2\alpha_1 y^7}{63(1+B)} - \frac{\alpha_1^2 y^8}{21(1+B)^2}\right] + Br(P-f)^4\left[\frac{\alpha_1^3 y^9}{18(1+B)^7} + \frac{\alpha_1^4 y^{10}}{270(1+B)^8}\right]$$

$$A_{18} = -\frac{Br(P-f)^4}{(1+B)^4}\left[\frac{h^6}{90} + \frac{2\alpha_1 h^7}{63(1+B)} - \frac{\alpha_1^2 h^8}{21(1+B)^2}\right] + Br(P-f)^4\left[\frac{\alpha_1^3 h^9}{18(1+B)^7} + \frac{\alpha_1^4 h^{10}}{270(1+B)^8}\right]$$

$$A_{19} = \frac{Br(P-f)^4}{(1+B)^4}\left[\frac{h^5}{15} + \frac{4\alpha_1 h^6}{18(1+B)} - \frac{8\alpha_1^2 h^7}{21(1+B)^2}\right] - Br(P-f)^4\left[\frac{12\alpha_1^3 h^8}{24(1+B)^7} + \frac{\alpha_1^4 h^9}{27(1+B)^8}\right]$$

$$A_{20} = \beta_2 A_{19} - A_{18}$$

$$G_1 = -Br(P-f)^2\left[\frac{y^4}{12(1+B)} + \frac{2\alpha_1 y^5}{20(1+B)^2}\right] - Br(P-f)^2\left[-\frac{\alpha_1^2 y^6}{30(1+B)^3} - \frac{\alpha_1^3 y^7}{42(1+B)^4}\right]$$

$$G_2 = -Br(P-f)^4\left[\frac{y^6}{90(1+B)^4} + \frac{2\alpha_1 y^7}{63(1+B)^5}\right] + \frac{Br(P-f)^4}{3(1+B)^6}\left[\frac{\alpha_1^2 y^8}{7} + \frac{\alpha_1^3 y^9}{6(1+B)} + \frac{\alpha_1^4 y^{10}}{90(1+B)^2}\right]$$

$$G_3 = Br^2(P-f)^4\left[-\frac{y^8}{288(1+B)^2} - \frac{29\alpha_1 y^9}{5040(1+B)^3}\right] + \frac{Br^2\alpha_1^4(P-f)^4}{10(1+B)^6}\left[\frac{191y^{12}}{19520} - \frac{\alpha_1^2 y^{14}}{315(1+B)^2}\right] + \frac{Br^2\alpha_1^2(P-f)^4}{180(1+B)^4}\left[-\frac{59\alpha_1 y^{11}}{77(1+B)} - \frac{\alpha_1^3 y^{13}}{7(1+B)^3}\right] + \frac{11Br^2\alpha_1^2(P-f)^4}{720(1+B)^4}y^{10}$$

$$G_4 = \frac{Br^2(P-f)^6}{90(1+B)^5}\left[\frac{y^{10}}{12} - \frac{139\alpha_1 y^{11}}{210(1+B)} - \frac{311\alpha_1^2 y^{12}}{105(1+B)^2}\right] + \frac{Br^2(P-f)^6}{30(1+B)^8}\left[\frac{139\alpha_1^3 y^{13}}{126} + \frac{3233\alpha_1^4 y^{14}}{5292(1+B)}\right] + \frac{Br^2(P-f)^6}{135(1+B)^{10}}\left[\frac{209\alpha_1^5 y^{15}}{245} + \frac{41\alpha_1^6 y^{16}}{210(1+B)}\right] + \frac{Br^2(P-f)^6}{(1+B)^{12}}\frac{\alpha_1^7 y^{17}}{11340}$$

$$G_5 = -Br(P-f)^2\left[\frac{h^4}{12(1+B)} + \frac{2\alpha_1 h^5}{20(1+B)^2}\right] - Br(P-f)^2\left[-\frac{\alpha_1^2 h^6}{30(1+B)^3} - \frac{\alpha_1^3 h^7}{42(1+B)^4}\right]$$

$$G_6 = -\frac{Br(P-f)^4}{(1+B)^4}\left[\frac{h^6}{90} + \frac{2\alpha_1 h^7}{63(1+B)} - \frac{\alpha_1^2 h^8}{21(1+B)^2}\right] - Br(P-f)^4\left[-\frac{\alpha_1^3 h^9}{18(1+B)^7} - \frac{\alpha_1^4 h^{10}}{270(1+B)^8}\right]$$

$$G_7 = Br^2(P-f)^4\left[-\frac{h^8}{288(1+B)^2} - \frac{29\alpha_1 h^9}{5040(1+B)^3}\right] + \frac{Br^2\alpha_1^4(P-f)^4}{10(1+B)^6}\left[\frac{191h^{12}}{19520} - \frac{\alpha_1^2 h^{14}}{315(1+B)^2}\right] + \frac{Br^2\alpha_1^2(P-f)^4}{180(1+B)^4}\left[-\frac{59\alpha_1 h^{11}}{77(1+B)} - \frac{\alpha_1^3 h^{13}}{7(1+B)^3}\right] + \frac{11Br^2\alpha_1^2(P-f)^4}{720(1+B)^4}h^{10}$$

$$G_8 = \frac{Br^2(P-f)^6}{90(1+B)^5}\left[\frac{h^{10}}{12} - \frac{139\alpha_1 h^{11}}{210(1+B)} - \frac{311\alpha_1^2 h^{12}}{105(1+B)^2}\right] + \frac{Br^2(P-f)^6}{30(1+B)^8}\left[\frac{139\alpha_1^3 h^{13}}{126} + \frac{3233\alpha_1^4 h^{14}}{5292(1+B)}\right] + \frac{Br^2(P-f)^6}{135(1+B)^{10}}\left[\frac{209\alpha_1^5 h^{15}}{245} + \frac{41\alpha_1^6 h^{16}}{210(1+B)}\right] + \frac{Br^2(P-f)^6}{(1+B)^{12}}\frac{\alpha_1^7 h^{17}}{11340}$$

$$G_9 = -Br(P-f)^2\left[\frac{h^3}{3(1+B)} + \frac{\alpha_1 h^4}{(1+B)^2}\right] - Br(P-f)^2\left[-\frac{\alpha_1^2 h^5}{5(1+B)^3} - \frac{\alpha_1^3 h^6}{6(1+B)^4}\right]$$

$$G_{10} = -\frac{Br(P-f)^4}{3(1+B)^4}\left[\frac{h^5}{5} + \frac{2\alpha_1 h^6}{3(1+B)} - \frac{8\alpha_1^2 h^7}{7(1+B)^2}\right] - Br(P-f)^4\left[-\frac{\alpha_1^3 h^8}{2(1+B)^7} - \frac{\alpha_1^4 h^9}{27(1+B)^8}\right]$$

$$G_{11} = Br^2(P-f)^4\left[-\frac{h^7}{3336(1+B)^2} - \frac{29\alpha_1 h^8}{560(1+B)^3}\right] + Br^2(P-f)^4\left[\frac{11\alpha_1^2 h^9}{720(1+B)^4} - \frac{59\alpha_1^3 h^{10}}{1260(1+B)^5}\right] + \frac{Br^2(P-f)^4}{(1+B)^6}\left[-\frac{\alpha_1^5 h^{12}}{1260(1+B)} - \frac{\alpha_1^6 h^{13}}{225(1+B)^2}\right] + +\frac{Br^2(P-f)^4}{(1+B)^6}\frac{191\alpha_1^4 h^{11}}{24600}$$

$$G_{12} = \frac{Br^2(P-f)^6}{3(1+B)^5}\left[\frac{h^9}{36} - \frac{1529\alpha_1 h^{10}}{6300(1+B)} - \frac{622\alpha_1^2 h^{11}}{525(1+B)^2}\right] + \frac{Br^2(P-f)^6 h^{12}\alpha_1^3}{3(1+B)^8}\left[\frac{3233\alpha_1 h}{3780(1+B)} + \frac{209\alpha_1^2 h^2}{735(1+B)^2}\right] + \frac{1807}{3780}\frac{Br^2(P-f)^6 h^{12}\alpha_1^3}{(1+B)^8} + \frac{Br^2(P-f)^6}{3(1+B)^{11}}\left[\frac{328\alpha_1^6 h^{15}}{4725} + \frac{17\alpha_1^7 h^{16}}{3780(1+B)}\right]$$

REFERENCES

[1] T. W. Latham, "Fluid motions in a peristaltic pump." Ph.D. dissertation, Massachusetts Institute of Technology, 1966.

[2] A. H. Shapiro, M. Y. Jaffrin, and S. L. Weinberg, "Peristaltic pumping with long wavelengths at low reynolds number," *Journal of Fluid Mechanics*, vol. 37, no. 4, pp. 799–825, 1969.

[3] T. Hayat, S. Hina, and N. Ali, "Simultaneous effects of slip and heat transfer on the peristaltic flow," *Communications in Nonlinear Science and Numerical Simulation*, vol. 15, no. 6, pp. 1526–1537, 2010.

[4] S. Shehzad, F. Abbasi, T. Hayat, F. Alsaadi, and G. Mousa, "Peristalsis in a curved channel with slip condition and radial magnetic field," *International Journal of Heat and Mass Transfer*, vol. 91, pp. 562–569, 2015.

[5] M. Javed, T. Hayat, M. Mustafa, and B. Ahmad, "Velocity and thermal slip effects on peristaltic motion of walters-b fluid," *International Journal of Heat and Mass Transfer*, vol. 96, pp. 210–217, 2016.

[6] M. Gudekote and R. Choudhari, "Slip effects on peristaltic transport of casson fluid in an inclined elastic tube with porous walls," *Journal of Advanced Research in Fluid Mechanics and Thermal Sciences*, vol. 43, no. 1, pp. 67–80, 2018.

[7] G. Manjunatha, R. Choudhari, K. Prasad, H. Vaidya, K. Vajravelu, and S. Sreenadh, "Peristaltic pumping of a casson fluid in a convectively heated porous channel with variable fluid properties," *Journal of Nanofluids*, vol. 8, no. 7, pp. 1446–1457, 2019.

[8] H. Vaidya, R. Choudhari, M. Gudekote, and K. V. Prasad, "Effect of variable liquid properties on peristaltic transport of rabinowitsch liquid in convectively heated complaint porous channel," *Journal of Central South University*, vol. 26, no. 5, pp. 1116–1132, 2019.

[9] R. Ellahi, M. M. Bhatti, and K. Vafai, "Effects of heat and mass transfer on peristaltic flow in a non-uniform rectangular duct," *International Journal of Heat and Mass Transfer*, vol. 71, pp. 706–719, 2014.

[10] Q. Hussain, S. Asghar, and A. Alsaedi, "Heat transfer analysis in peristaltic slip flow with hall and ion-slip currents," *Scientia Iranica*, vol. 23, no. 6, pp. 2771–2783, 2016.

[11] F. Salah and M. H. Elhafian, "Numerical solution for heat transfer of non-newtonian second-grade fluid flow over stretching sheet via successive linearization method," *IAENG International Journal of Applied Mathematics*, vol. 49, no. 4, pp. 505–512, 2019.

[12] G. Manjunatha, C. Rajashekhar, H. Vaidya, K. Prasad, and K. Vajravelu, "Impact of heat and mass transfer on the peristaltic mechanism of jeffery fluid in a non-uniform porous channel with variable viscosity and thermal conductivity," *Journal of Thermal Analysis and Calorimetry*, vol. 139, no. 2, pp. 1213–1228, 2020.

[13] H. Vaidya, C. Rajashekhar, M. Gudekote, and K. Prasad, "Heat transfer and slip consequences on peristaltic transport of a casson fluid in an axisymmetric porous tube," *Journal of Porous Media*, vol. 24, no. 3, pp. 77–94, 2021.

[14] B. Ahmed, T. Hayat, and A. Alsaedi, "Mixed convection peristalsis of hybrid nanomaterial flow in thermally active symmetric channel," *Case Studies in Thermal Engineering*, vol. 27, 2021.

[15] R. Choudhari, F. Mebarek-Oudina, H. F. Öztop, H. Vaidya, and K. V. Prasad, "Electro-osmosis modulated peristaltic flow of non-newtonian liquid via a microchannel and variable liquid properties," *Indian Journal of Physics*, pp. 1–14, 2022.

[16] T. K. Mittra and S. N. Prasad, "On the influence of wall properties and poiseuille flow in peristalsis," *Journal of Biomechanics*, vol. 6, no. 6, pp. 681–693, 1973.

[17] T. Hayat, S. Hina, A. A. Hendi, and S. Asghar, "Effect of wall properties on the peristaltic flow of a third grade fluid in a curved channel with heat and mass transfer," *International Journal of Heat and Mass Transfer*, vol. 54, no. 23–24, pp. 5126–5136, 2011.

[18] M. Mustafa, S. Hina, T. Hayat, and A. Alsaedi, "Influence of wall properties on the peristaltic flow of a nanofluid: analytic and numerical solutions," *International Journal of Heat and Mass Transfer*, vol. 55, no. 17–18, pp. 4871–4877, 2012.

[19] M. Javed, T. Hayat, and A. Alsaedi, "Effect of wall properties on the peristaltic flow of a non-newtonian fluid," *Applied Bionics and Biomechanics*, vol. 11, no. 4, pp. 207–219, 2014.

[20] S. Hina, M. Mustafa, T. Hayat, and N. D. Alotaibi, "On peristaltic motion of pseudoplastic fluid in a curved channel with heat/mass transfer and wall properties," *Applied Mathematics and Computation*, vol. 263, pp. 378–391, 2015.

[21] Z. Nisar, T. Hayat, A. Alsaedi, and B. Ahmad, "Wall properties and convective conditions in mhd radiative peristalsis flow of eyring–powell nanofluid," *Journal of Thermal Analysis and Calorimetry*, vol. 144, no. 4, pp. 1199–1208, 2021.

[22] A. Tanveer, T. Hayat, and A. Alsaedi, "Variable viscosity in peristalsis of sisko fluid," *Applied Mathematics and Mechanics*, vol. 39, no. 4, pp. 501–512, 2018.

[23] G. Manjunatha, C. Rajashekhar, H. Vaidya, K. Prasad, and O. D. Makinde, "Effects wall properties on peristaltic transport of rabinowitsch fluid through an inclined non-uniform slippery tube," in *Defect and Diffusion Forum*, vol. 392. Trans Tech Publ, 2019, pp. 138–157.

[24] K. V. Prasad, H. Vaidya, G. Manjunatha, K. Vajravelu, C. Rajashekhar, and V. Ramanjini, "Influence of variable transport properties on casson nanofluid flow over a slender riga plate: Keller box scheme," *Journal of Advanced Research in Fluid Mechanics and Thermal Sciences*, vol. 64, no. 1, pp. 19–42, 2019.

[25] C. Rajashekhar, F. Mebarek-Oudina, H. Vaidya, K. Prasad, G. Manjunatha, and H. Balachandra, "Mass and heat transport impact on the peristaltic flow of a ree–eyring liquid through variable properties for hemodynamic flow," *Heat Transfer*, vol. 50, no. 5, pp. 5106–5122, 2021.

[26] C. Rajashekhar, F. Mebarek-Oudina, I. E. Sarris, H. Vaidya, K. V. Prasad, G. Manjunatha, and H. Balachandra, "Impact of electroosmosis and wall properties in modelling peristaltic mechanism of a jeffrey liquid through a microchannel with variable fluid properties," *Inventions*, vol. 6, no. 4, pp. 1–21, 2021.

[27] R. E. Powell and H. Eyring, "Mechanisms for the relaxation theory of viscosity," *Nature*, vol. 154, no. 3909, pp. 427–428, 1944.

[28] N. S. Akbar and S. Nadeem, "Characteristics of heating scheme and mass transfer on the peristaltic flow for an eyring–powell fluid in an endoscope," *International Journal of Heat and Mass Transfer*, vol. 55, no. 1–3, pp. 375–383, 2012.

[29] F. Abbasi, A. Alsaedi, and T. Hayat, "Peristaltic transport of eyring-powell fluid in a curved channel," *Journal of Aerospace Engineering*, vol. 27, no. 6, 2014.

[30] S. Hina, "Mhd peristaltic transport of eyring–powell fluid with heat/mass transfer, wall properties and slip conditions," *Journal of Magnetism and Magnetic Materials*, vol. 404, pp. 148–158, 2016.

[31] S. Farooq, T. Hayat, B. Ahmad, and A. Alsaedi, "Mhd flow of eyring–powell liquid in convectively curved configuration," *Journal of the Brazilian Society of Mechanical Sciences and Engineering*, vol. 40, no. 3, pp. 1–14, 2018.

[32] F. M. Elniel, S. Mustafa, A. Bahar, Z. A. Aziz, and F. Salah, "Effects of shear stress on magnetohydrodynamic (mhd) powell eyring fluid over a porous plate: A lift and drainage problem," *IAENG International Journal of Applied Mathematics*, vol. 51, no. 4, pp. 851–860, 2021.